

Norrin stimulates cell proliferation in the superficial retinal vascular plexus and is pivotal for the recruitment of mural cells

Jurian Zuercher^{1,2,†}, Martin Fritzsche^{1,†}, Silke Feil¹, Lucas Mohn^{1,2} and Wolfgang Berger^{1,2,3,*}

¹Institute of Medical Molecular Genetics, ²Neuroscience Center Zurich (ZNZ) and ³Center for Integrative Human Physiology (ZIHP), University of Zurich, Zurich, Switzerland

Received January 20, 2012; Revised and Accepted February 28, 2012

Mutations in Norrin, the ligand of a receptor complex consisting of FZD4, LRP5 and TSPAN12, cause severe developmental blood vessel defects in the retina and progressive loss of the vascular system in the inner ear, which lead to congenital blindness and progressive hearing loss, respectively. We now examined molecular pathways involved in developmental retinal angiogenesis in a mouse model for Norrie disease. Comparison of morphometric parameters of the superficial retinal vascular plexus (SRVP), including the number of filopodia, vascular density and number of branch points together with inhibition of Notch signaling by using DAPT, suggest no direct link between Norrin and Notch signaling during formation of the SRVP. We noticed extensive vessel crossing within the SRVP, which might be a loss of Wnt- and MAP kinase-characteristic feature. In addition, endomucin was identified as a marker for central filopodia, which were aligned in a thorn-like fashion at P9 in Norrin knockout (*Ndp*^{−/−}) mice. We also observed elevated mural cell coverage in the SRVP of *Ndp*^{−/−} mice and explain it by an altered expression of *PDGFβ* and its receptor (*PDGFRβ*). *In vivo* cell proliferation assays revealed a reduced proliferation rate of isolectin B4-positive cells in the SRVP from *Ndp*^{−/−} mice at postnatal day 6 and a decreased mitogenic activity of mutant compared with the wild-type Norrin. Our results suggest that the delayed outgrowth of the SRVP and decreased angiogenic sprouting in *Ndp*^{−/−} mice are direct effects of the reduced proliferation of endothelial cells from the SRVP.

INTRODUCTION

Mutations in the human *NDP* (Norrie disease pseudoglioma) gene, encoding Norrin, cause congenital blindness, progressive deafness and mental retardation, a triad of symptoms characteristic for Norrie disease (ND) (1–5). Alternatively, mutations in *NDP* can exclusively lead to ocular symptoms in X-linked exudative vireoretinopathy (EVR) (6), Coats' disease and retinopathy of prematurity (7,8). EVR is also caused by mutations in Frizzled-4 (*FZD4*, *FZD4*), low-density lipoprotein receptor-related protein 5 (*LRP5*, *LRP5*) or tetraspanin-12 (*TSPAN12*, *TSPAN12*) (9–11). Recessive mutations in *LRP5* may also cause osteoporosis pseudoglioma syndrome (OPPG), which manifests with low bone mass in addition to the ocular phenotype in patients (OMIM: #259770). It has been shown *in vitro* that Norrin is a ligand

for the canonical Wnt signaling receptor complex consisting of FZD4, LRP5 and TSPAN12 (12,13). Furthermore, the outgrowth of the superficial retinal vascular plexus (SRVP) from *Ndp*^{−/−}, *Fzd4*^{−/−}, *Lrp5*^{−/−} and *Tspan12*^{−/−} is delayed and incomplete and all of these knockout mice lack the deep and intermediate retinal vascular plexuses (12–16). We generated and examined a Norrin knockout mouse model (*Ndp*^{−/−}) that resembles the human Norrie disease phenotype with respect to blindness and hearing loss (4,14,17). Hyaloid vessels do not completely regress in *Ndp*^{−/−}, *Fzd4*^{−/−}, *Lrp5*^{−/−} and *Tspan12*^{−/−} knockout mice (12–14,16). Retinal vascular hemorrhage and exudation from retinal blood vessels in *Ndp* knockout mice (*Ndp*^{−/−}) are characteristic features. We previously demonstrated that expression of the plasmalemma vesicle-associated protein (PLVAP), which mediates vascular fenestration and promotes vascular leakiness, is highly

*To whom correspondence should be addressed at: Schorenstrasse 16, CH-8603 Schwerzenbach. Tel: +41 446557031; Fax: +41 446557213; Email: berger@medmolgen.uzh.ch

†These two authors contributed equally.

upregulated in *Ndp^{y/-}* retinas (18). Upregulation of PLVAP/MECA32 in retinal endothelial cells (ECs) has also been shown for *Lrp5^{-/-}* and *Tspan12^{-/-}* mice (13). Furthermore, it was shown that upregulation of PLVAP indicates the loss of canonical Wnt signaling (19). The delayed outgrowth of the SRVP and the absence of deep sprouting could be caused either by defects in sprouting angiogenesis or by reduced proliferation of the SRVP. Sprouting angiogenesis is mediated by endothelial tip cells that guide the growing SRVP from the optic nerve head towards the retinal periphery along a vascular endothelial growth factor (VEGF) gradient (20). Stalk cells following tip cells divide ensuring proliferation and growth. Thus, an imbalance of tip and stalk cells could lead to both observed effects. The proper differentiation of tip and stalk cells is mediated by a balanced expression and interaction of Notch1 with its ligands Dll4 and Jagged1 (21–23). Dll4 is expressed in tip cells and induces Notch signaling in adjacent stalk cells. In contrast, Jagged1 is expressed in stalk cells impeding Notch signaling in adjacent tip cells. Disruption of Notch signaling has been shown to alter morphometric parameters, such as the number of peripheral tip cell filopodia, vascular density and the number of vascular branch points. The outgrowth of the SRVP along the VEGF gradient involves MAPK signaling. VEGF, provided by astrocytes or retinal ganglion cells, binds a receptor complex consisting of VEGF receptor 2 (VEGFR2) and neuropilin 1 (Nrp1) activating downstream MAPK signaling. Loss of the cytoplasmic Nrp1 domain (Nrp1^{cytoΔ/Δ}) or nestin-specific knockout of VEGF (VEGF_{NES-CRE}) in mice causes artery/vein crossing (A/V crossing) in the SRVP of these mice. VEGF_{NES-CRE} mice additionally show aberrant deep sprouting (24,25).

Here, we focused on defects during development of the SRVP in *Ndp^{y/-}* mice. We quantified several vascular and angiogenic parameters and observed extensive vessel crossing within the SRVP which might be a MAPK-characteristic feature. We found reduced cell proliferation in the SRVP at the vascular front at P6 in *Ndp^{y/-}* mice which may explain the delayed outgrowth of the SRVP. We also detected elevated mural cell (MC) coverage of the SRVP starting at P9, which is consistent with previously found upregulation of *Tie1*, *Pdgfrβ* and *Pdgfrβ*. Finally, we report for the first time endomucin-positive supernumerary central filopodia of the SRVP in *Ndp^{y/-}* retinas culminating at P9, the time point when the deep retinal vascular plexus (DRVP) normally would develop.

RESULTS

Vascular development in Norrin knockout mice

The wild-type mouse retina is avascular at birth and outgrowth of the SRVP progresses from the center towards the periphery from P1 until P8. Because the outgrowth of the SRVP is incomplete and delayed in *Ndp^{y/-}* mice (14), we hypothesized that there might be an imbalance between tip cell filopodia and/or adjacent stalk cell proliferation. We quantified the number of filopodia as well as the vascular density and number of branch points in the central plexus at the vascular front at P5 and P7 (Fig. 1) (Supplementary Material, Table S1). The number of filopodia was significantly increased but the vascular density (Fig. 1A, C, E, G, I, K) and the

number of branch points (Fig. 1A, C, E, G, J, L) were significantly decreased at P5 and P7 in *Ndp^{y/-}* mice. Moreover, filopodial protrusions in *Ndp^{y/-}* mice are straighter and expand with a narrower angle than filopodia of wild-type littermates (Fig. 1O) (Supplementary Material, Table S2). In contrast to the increased number of filopodia, the vascular front in general appears to be less ramified with a reduced amount of long tip cell protrusions (Fig. 1B and F).

Comparison of vascular development in different mouse models

Available morphometric data from three Norrin-Wnt signaling knockout mice (*Fzd4^{-/-}*, *Lrp5^{-/-}* and *Tspan12^{-/-}*), three Notch signaling knockout mice (*Dll4^{+/-}*, *Jag1^{iΔEC}*, *Nrarp^{-/-}*), *Ang2^{LZ/LZ}* and Pax6 dependent hypoxia inducible factor 1 α (*HIF1 α ^{ΔPax6}*) knockout mice were compared (Table 1). The morphometric comparison of *Jag1^{iΔEC}* with *Ndp^{y/-}* mice was of special interest since *Jag1* has been shown to be a canonical Wnt target gene in hair follicle cells comprising two LEF/TCF-binding sites within its promoter region (26,27). We compared our morphometric data from Norrin KO mice with published morphometric data from *Jag1^{iΔEC}* mice and recognized delayed and incomplete outgrowth of the SRVP, together with a reduced vascular density and a decreased number of branch points in *Jag1^{iΔEC}* and *Ndp^{y/-}* mice. In contrast to *Ndp^{y/-}* mice, the number of tip cell filopodia was reduced in *Jag1^{iΔEC}* mice. *Dll4^{+/-}* mice have an increased number of filopodia, increased number of branchpoints and a denser vascular SRVP. Hence, the *Ndp^{y/-}* phenotype of the SRVP displays as an intermingled picture, with a peripheral *Jag1* gain of function but central *Jag1* loss of function features. We asked the question whether or not Norrin is a negative regulator of Notch signaling. To answer this question, we examined the effect of Notch inhibition in *Ndp^{y/-}* mice in order to see if this may rescue the abnormal vascular development. We quantified and compared morphometric parameters in Norrin knockout and wild-type mice after inhibition of Notch signaling by injection of the γ -secretase inhibitor DAPT (Fig. 2). Administration of DAPT increased vascular density in wild-type and *Ndp^{y/-}* mice (Fig. 2A–E), while the number of filopodia only increased in wild-type but not in *Ndp^{y/-}* retinas (Fig. 2F–J) (Supplementary Material, Table S3).

Retinal EC proliferation in Norrin-deficient mice

To test the hypothesis if Norrin acts as a mitogen for cells in the SRVP, which would explain the reduced vascular density as well as the delayed and incomplete radial vascular outgrowth in *Ndp^{y/-}* mice, we quantified central EC proliferation after systemic bromodeoxyuridine (BrdU) injection and found significantly reduced proliferation rates of isolectin B4 (IB4)-positive ECs from the SRVP in *Ndp^{y/-}* mice at P6 (WT: ME \pm SD 101.71 \pm 16.54; KO: ME \pm SD 52.17 \pm 9.62; *P*-value: 1.8E–5) (Fig. 3A and C). The only exceptions from this observation are local hotspots of proliferation within bulky unorganized regions at the vascular front (Fig. 3D). Additionally, we monitored the effect of Norrin on cell cycle progression in cell culture experiments by using an

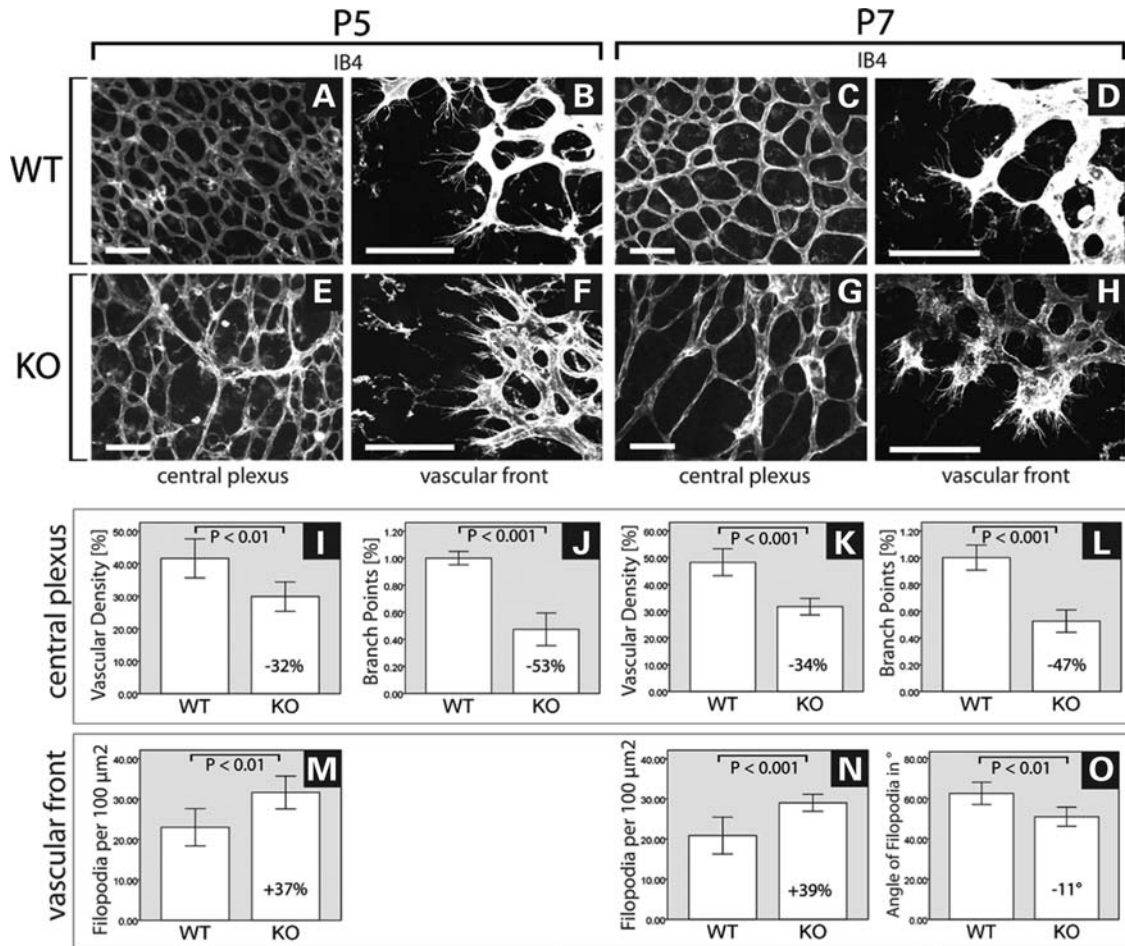


Figure 1. Morphometric parameters in Norrin knockout versus wild-type mice. $Ndp^{y/-}$ mice show decreased vascular density, a decreased number of branch points but supernumerary filopodia, which are aligned in a more narrow angle compared with wild-type mice at P5 and P7. (A, E, C, G) Representative central retinal whole-mounts from wild-type (WT) and $Ndp^{y/-}$ (KO) retinas stained with IB4. (B, D, F, H) Representative peripheral retinal whole-mounts from WT and $Ndp^{y/-}$ retinas stained with IB4. Emerging filopodia are visible. Quantification of vascular density (I and K), number of branch points (J and L), number of filopodia (M and N) and angle of filopodia (O). Average and confidence intervals are shown. P -values below $\alpha = 0.05$ were considered statistically significant. Scale bars = 100 μm .

E2F transcription factor-mediated reporter assay (cell proliferation controlling transcription factor-dependent luciferase reporter construct, reviewed in 28). For this, we transiently transfected pE2F luciferase reporter constructs into HEK293T cells which ectopically express the same amount of either human wild-type or a pathogenic variant of Norrin containing the p.C95R mutation (Supplementary Material, Fig. S1), which has been associated with the classic picture of Norrie disease (29). HEK293T cells do not endogenously express Norrin, but were positive in RT-PCR for transcripts from *FZD4*, *LRP5* and *TSPAN12* (Supplementary Material, Fig. S1). Similarly to our BrdU data in $Ndp^{y/-}$ mice, we found almost 6-fold increased cell cycle progression in cells that stably express human wild-type Norrin compared with cells that express the mutant Norrin isoform (Fig. 3F, Supplementary Material, Table S4).

Vascular remodeling in Norrin-deficient mice

Despite the reduced vascular outgrowth of the SRVP, we occasionally noticed bulky vascular areas at the front of

$Ndp^{y/-}$ mice, comprising three-dimensional accumulations of ECs (Fig. 4D). To monitor vascular remodeling across the plexus, retinal whole-mounts were double stained for IB4 and collagen IV (ColIV). ColIV-positive tubes lacking IB4 staining represent empty basement membrane sleeves at positions where blood vessels have regressed (30,31). We noticed that vascular remodeling was elevated in $Ndp^{y/-}$ mice at peripheral bulky vascular areas of the SRVP, but not in central areas (Fig. 4C, white dots). Furthermore, we noticed vessel-crossing in $Ndp^{y/-}$ retinas. Vessels that morphologically resemble veins [venous character (VC)] cross and grow below vessels that resemble arteries [arterial character (AC)] between P7 and P21 (A/V crossing) (Fig. 5, Supplementary Material, Fig. S3). ACs in Norrin knockout mice also interconnect less to the central plexus compared with the wild-type and instead grow further into the periphery (Fig. 6D). At P21, disorganized twisted and tangled blood vessels form above the superficial plexus resembling fibrosis (Supplementary Material, Fig. S3t and w). We hypothesized that A/V crossing could be caused by altered astrocyte-EC interaction and therefore co-stained astrocytes against PDGFR α and blood

Table 1. Morphometric data among mutant mice with comparable retinal vascular phenotype

	<i>Ndp</i> ^{-/-}	<i>Fzd4</i> ^{-/-}	<i>Lrp5</i> ^{-/-}	<i>Tspan12</i> ^{-/-}	<i>Dll4</i> ^{+/-}	<i>Jag1</i> ^{iΔEC}	<i>Nrarp</i> ^{-/-}	<i>Ang2</i> ^{LZ/LZ}	<i>HIF1α</i> ^{ΔPAX6}
Pathway affected	Canonical Wnt-signaling	Canonical Wnt-signaling	Canonical Wnt-signaling	Canonical Wnt-signaling	Notch signaling	Notch signaling; tamoxifen-induced EC-specific deletion	Notch, β-catenin/ Lef1-dependent Wnt signaling	Tie2 signaling; LZ = lacZ	Hypoxia
Vascular outgrowth of SRVP	Delayed and incomplete	Delayed and incomplete	Delayed and incomplete	Delayed and incomplete	Delayed	Delayed (-44%)	Delayed but complete	Periphery remains avascular	Not delayed nor reduced
Vascular density of SRVP	Reduced (-34%, P7)	Not available	Not available	Reduced	Increased (+58% ^a)	Reduced (-32%, P6)	Reduced at P5 but not different in adult	Not available	Not available
Number of branch points of SRVP	Reduced (-47%, P7)	Not available	Not available	Not available	Increased (+96% ^a)	Reduced (-65%, P6)	Reduced at P5 but not different in adult	Not available	Not available
Number of filopodia of SRVP	Increased (+39%, P7)	Not available	Not available	Not available	Increased (sprouts increased +63% ^a)	Reduced (-27%, P6)	Not different at P5	Not available	Not available
A/V crossing in SRVP till P7	Present	Present	Present	Present	Absent	Absent	Present	Not deducible due to picture quality	Absent
DRVP	Absent	Absent	Absent	Absent	Present	Present	Present	Absent	Present
Intermediate retinal vascular plexi	Absent	Absent	Absent	Absent	Present	Present	Present	Absent	Absent
References	Luhmann <i>et al.</i> (14), this work	Xu <i>et al.</i> (12)	Xia <i>et al.</i> (16,41) and Chen <i>et al.</i> (42)	Junge <i>et al.</i> (13)	Lobov <i>et al.</i> (21)	Benedito <i>et al.</i> (22)	Phng <i>et al.</i> (43)	Gale <i>et al.</i> (44)	Caprara <i>et al.</i> (45)

^a% estimated from graph.

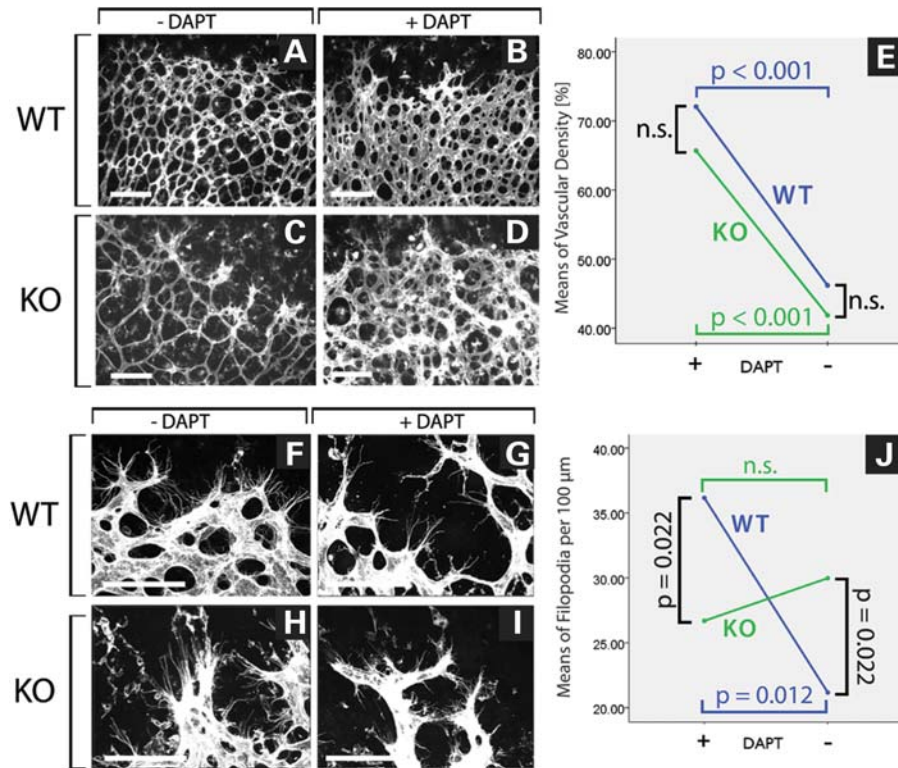


Figure 2. Effects of Notch signaling inhibition in wild-type and Norrin knockout mice. Pharmacological administration of DAPT increases vascular density at the vascular front in wild-type and *Ndp^{y/y}* mice. The number of filopodia only increases in wild-type but not in *Ndp^{y/y}* mice upon DAPT treatment. (A–D) Representative retinal whole-mounts stained with IB4 48 h after DAPT injection in P7 wild-type (WT) and *Ndp^{y/y}* (KO) animals. (E) Statistical analysis shows that peripheral vascular density increases in both genotypes upon DAPT treatment. (F–I) Representative retinal whole-mounts of IB4 staining 48 h after DAPT treatment of P7 wild-type (WT) and *Ndp^{y/y}* (KO) animals. Filopodia at the vascular front are visible. (J) Statistical analysis shows that number of filopodia increases only after DAPT treatment in the WT but not in *Ndp^{y/y}* mice. *P*-values below $\alpha = 0.05$ were considered statistically significant. Scale bars = 100 μ m.

vessels with IB4 (Supplementary Material, Fig. S2). We did not observe an altered astrocytic network in *Ndp^{y/y}* retinas compared with wild-type and alignment between astrocytes and ECs was normal.

Mice lacking the *Nrp1* cytoplasmatic domain or *VEGF_{NES-CRE}* mice also show A/V crossing in the SRVP (24,25). This suggests that the loss of MAPK signaling might cause this phenotype. Therefore, we made use of our stably wild-type or p.C95R Norrin expressing HEK293T cell lines (Supplementary Material, Fig. S1) to monitor MAPK activity. We found a 1.9-fold increase in MAPK signaling in cells that express wild-type Norrin compared with those that expressed the mutant, disease-associated variant (Fig. 5I, Supplementary Material, Table S5).

Because of the above-described, strong SRVP phenotype in *Ndp^{y/y}* mice, it was crucial to examine whether the VCs and ACs exhibit characteristic molecular features of the respective vessel types. Retinal flatmounts were stained either for endomucin or for smooth muscle actin (SMA) at P7, P9, P12 and P21. In both, wild-type and *Ndp^{y/y}* mice, endomucin stained veins and venous portions while staining of arteries and arterioles was less intense (Fig. 6, Supplementary Material, Fig. S4) (32,33). Interestingly, the endomucin staining revealed super-numerary thorn-like assembled central filopodia around veins and capillaries of *Ndp^{y/y}* retinas (Fig. 6D and E). In contrast, capillary sprouts were much less abundant and, if present,

much shorter in wild-type mice. Staining for the arterial and MC marker α -SMA in wild-type mice specifically labeled arteries at P7, P9 and P12 as well as arteries and large veins at P21. In *Ndp^{y/y}* retinas, arteries, veins and capillaries were covered with SMA-positive cells at P9, P12 and P21 (Fig. 7, Supplementary Material, Fig. S5). Thus, MC recruitment to the SRVP is abnormally increased in *Ndp^{y/y}* retinas.

DISCUSSION

Deficiency of Norrin is known to cause Norrie disease, a severe X-linked recessive human disease characterized by congenital blindness, progressive hearing loss and, in some patients, mental retardation. We made use of a mouse model which mimics the human disease in eye and ear and applied morphometric analyses, Notch-inhibition by DAPT administration, as well as cell proliferation assays to characterize the angiogenic processes in the retina. We provide evidence that Norrin is a mitogenic stimulus for cells in the SRVP. Consistently, wild-type Norrin promotes E2F transcription factor-mediated cell cycle progression in a cell culture assay. Further, we identified endomucin as a marker for central filopodia, which were aligned in a thorn-like fashion at P9 in *Ndp^{y/y}* mice. Finally, we found aberrant vascular SMA-positive MC coverage of veins and capillaries in the SRVP

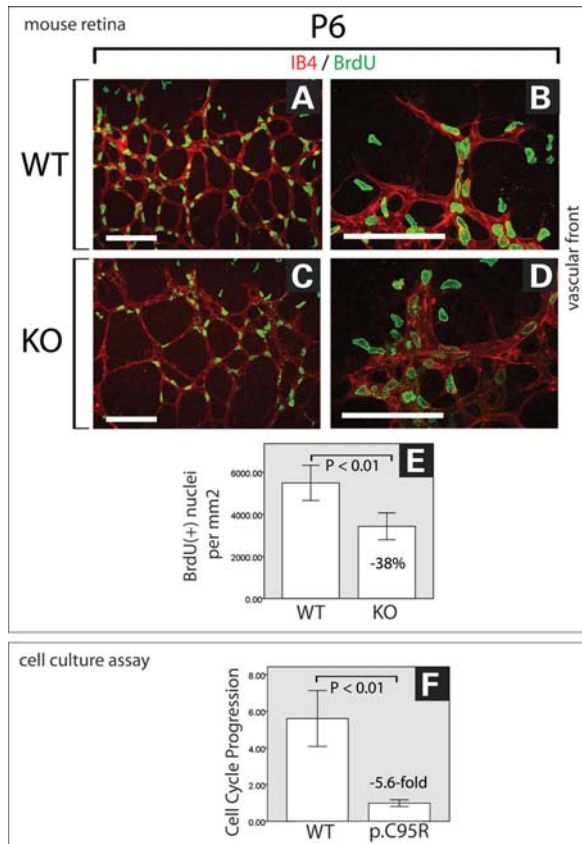


Figure 3. Decreased proliferation rate of ECs in Norrin knockout mice and reduced cell cycle progression due to a mutation (p.C95R) in human Norrin. Overall proliferation is reduced in *Ndp*^{y/y} mice at P6. Representative retinal whole-mounts of wild-type (WT) (A and B) and *Ndp*^{y/y} mice (KO) (C and D) were stained for blood vessels with IB4 (red) and for proliferating cells after BrdU incorporation (green). (D) Local hotspots of proliferation within thickened areas of the vascular front are occasionally seen in *Ndp*^{y/y} mice and were excluded from quantification of proliferation. (E) Quantification of proliferating vascular ECs after BrdU-incorporation revealed a reduced proliferation rate (-38%) in *Ndp*^{y/y} mice. (F) Expression of wild-type Norrin (WT) leads to 5.6-fold increase in the proliferation rate in HEK293T cells compared with cells expressing a mutant (p.C95R) human Norrin. Average and confidence intervals are shown. *P*-values below $\alpha = 0.05$ were considered statistically significant. Scale bars = 100 μ m.

in *Ndp*^{y/y} mice which indicates abnormally increased MC recruitment of the SRVP from Norrin KO mice.

Norrin and Notch signaling are not directly linked

We examined features of the SRVP in *Ndp*^{y/y} mice by quantifying and comparing morphometric parameters (Figs 1 and 2, Supplementary Material, Tables S1–S3) with published data from different mouse models with retinal vascular phenotypes (Table 1). We did not quantify later stages than P7 since the outgrowth of the superficial plexus in wild-type mice ends soon after this stage of development.

We noticed that the outgrowth of the SRVP is delayed in all mouse models (Table 1), but incomplete vascular outgrowth was only observed in mutants with disrupted canonical Wnt signaling (*Ndp*^{y/y}, *Fzd4*^{-/-} and *Lrp5*^{-/-}). Both the deep

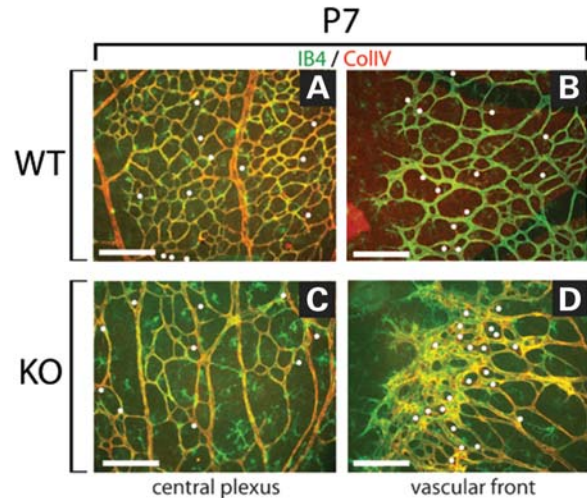


Figure 4. Massive vessel regression at the bulky vascular front in *Ndp*^{y/y} mice at P7. IB4 (green) and ColIV (red) co-stained retinal whole-mounts from wild-type (WT) (A and B) and *Ndp*^{y/y} mice (KO) (C and D). ColIV+, IB4-stainings represent empty membrane sleeves, where blood vessels have regressed (white dots). Regression was increased at the bulky vascular front in *Ndp*^{y/y} retinas (D). Scale bars = 100 μ m.

and intermediate retinal vascular plexuses (DRVP, IRVP) are absent in mice with deficient Wnt signaling components (*Ndp*^{y/y}, *Fzd4*^{-/-}, *Lrp5*^{-/-} and *Tspan12*^{-/-}) and in *Ang2*^{LZ/LZ} mice, but not in Notch signaling deficient mice (*Dll4*^{+/-} or *Jag1* ^{Δ EC}). The intermediate plexus is absent in *HIF1 α* ^{Δ Pax6} mice, while the deep plexus is present (Table 1). We hypothesized that the canonical Wnt target gene *Jag1* might link Norrin-Wnt and Notch signaling during development of the SRVP, since knocking out *Ndp* or *Jag1* leads to aberrant SRVP development. However, we found significant differences in morphometric parameters between *Ndp*^{y/y} and *Jag1* ^{Δ EC} retinas, which are in conflict with this hypothesis. The number of filopodia was increased in *Ndp*^{y/y} and reduced *Jag1* ^{Δ EC} mice. *Jag1* ^{Δ EC} retinas also do not display defects in deep vascular development (22) which is a characteristic feature in *Ndp*^{y/y} retinas. All these phenotypic differences suggest that there is no direct link between Norrin-Wnt and Notch signaling via *Jag1*.

Inhibiting Notch signaling through systemic DAPT administration led to an increased vascular density in *Ndp*^{y/y} mice, but it did not reduce the supernumerary filopodia. Furthermore, vascular density increased similarly in wild-type and *Ndp*^{y/y} retinas after DAPT treatment, excluding a synergistic effect (Fig. 2E). Accordingly, interaction effects were rejected by univariate analysis of variance (data not shown). Although the peripheral vascular network at the front is denser in DAPT-treated *Ndp*^{y/y} mice (Fig. 2D), it still seems disorganized, three-dimensional and not planar. This implies that Notch inhibition can induce a peripheral hyper angiogenic response in *Ndp*^{y/y} mice but not re-establish normal vascular development. The diameter of the peripheral blood vessels increased, which might be due to involvement of Dll4-Notch signaling in A/V differentiation, leading to a more pronounced venous phenotype after DAPT injection and to an increase in vessel diameter (Fig. 2A–D). The number of filopodia significantly

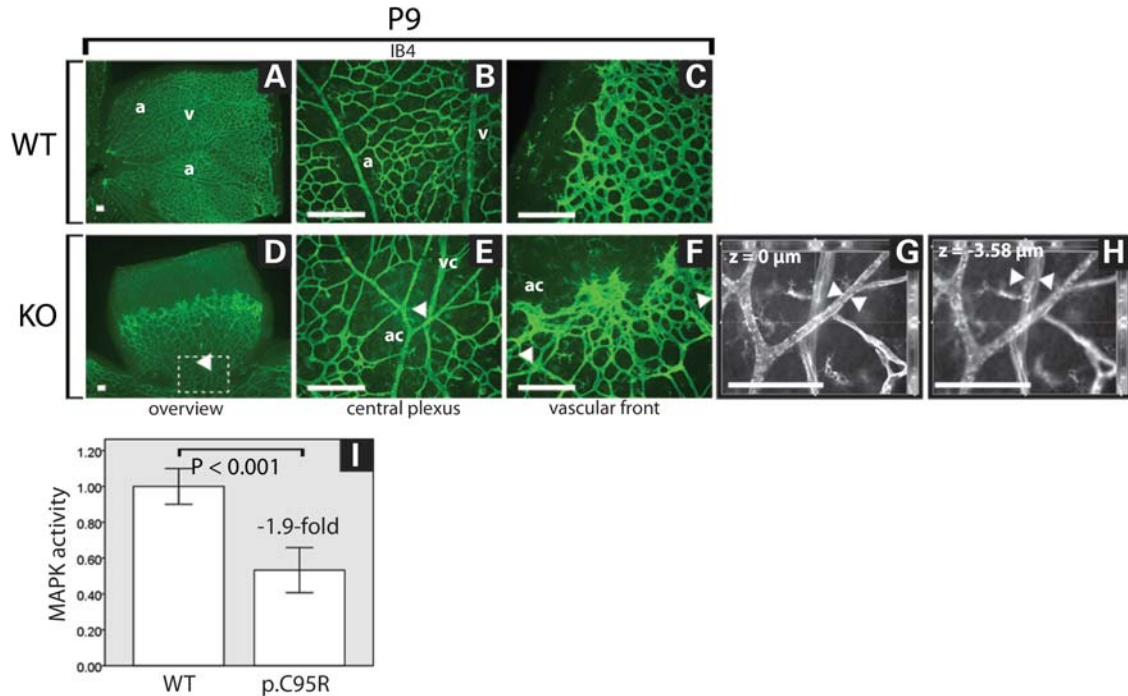


Figure 5. Blood vessel crossing in Norrin knockout mice. Arteries and veins often cross each other in *Ndp*^{−/−} retinas. Retinal whole-mounts of wild-type (WT) (A–C) and *Ndp*^{−/−} mice (KO) (D–H) were stained with IB4 to label blood vessels (green A–F, or grey G + H). We noticed abundant A/V crossings at the center (E, arrowheads) and periphery (F, arrowheads) of the SRVP from *Ndp*^{−/−} retinas. Note, that (E) represents the box indicated in (D). (G) and (H) are confocal images from the blood vessels marked in (E), focused on the upper artery (G), and on the lower vein (H). The distance between both vessels is 3.58 μm . (I) Ectopic expression of wild-type Norrin (WT) leads to 1.9-fold increase in MAPK signaling in HEK293T cells compared with cells expressing a mutant (p.C95R), disease-associated human Norrin. a, artery; ac, arterial character; v, vein; vc, venous character. Scale bars = 100 μm .

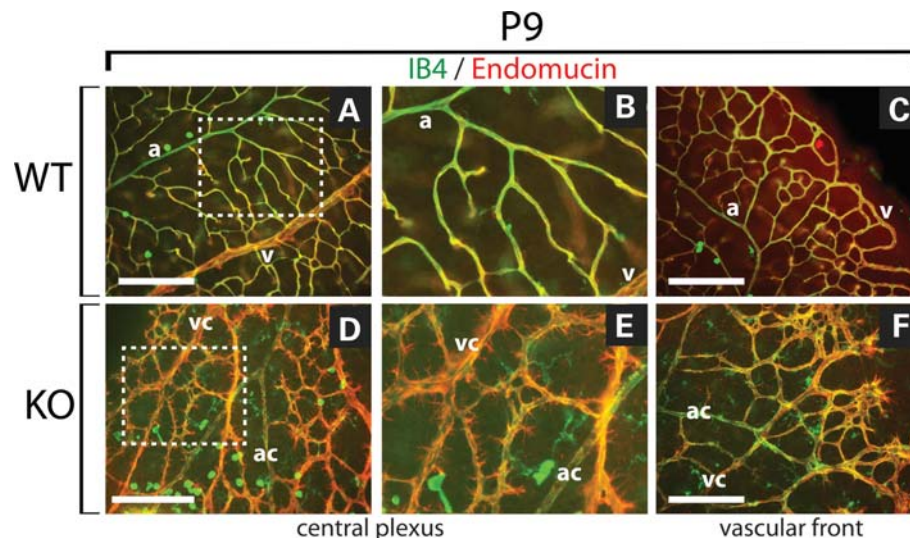


Figure 6. Large central filopodia in *Ndp*^{−/−} mice at P9. Retinal whole-mounts from wild-type (WT) (A–C) and *Ndp*^{−/−} mice (KO) (D–F) were co-stained with IB4 (green) to label blood vessels and with endomucin (red) which preferentially stains veins, venous vessels and central filopodia. (B) represents box in (A) and (E) represents box in (D). Endomucin staining revealed that vessels with a venous character (vc) but not with an arterial character (ac) are laced with super-numerary central filopodia. a, artery; v, vein. Scale bars = 100 μm .

increased in wild-type mice, but was unaltered in *Ndp*^{−/−} retinas upon DAPT administration (Fig. 2G, I, J).

Vascular remodeling in Norrin-deficient mice

We found enhanced vascular proliferation (Fig. 3) and also enhanced vascular regression/remodeling (Fig. 4) at the

vascular bulky front in *Ndp*^{−/−} mice after BrdU injection and by co-staining of CollIV and IB4. We interpret the vessel regression of *Ndp*^{−/−} retinas as secondary effect which ensures a planar vascular plexus at positions where bulky vascular fronts were present before moving towards the periphery. Disorganized vascular fronts are also present in *Fzd4*^{−/−}, *Lrp5*^{−/−} and *Tspan12*^{−/−} retinas (12,13,34).

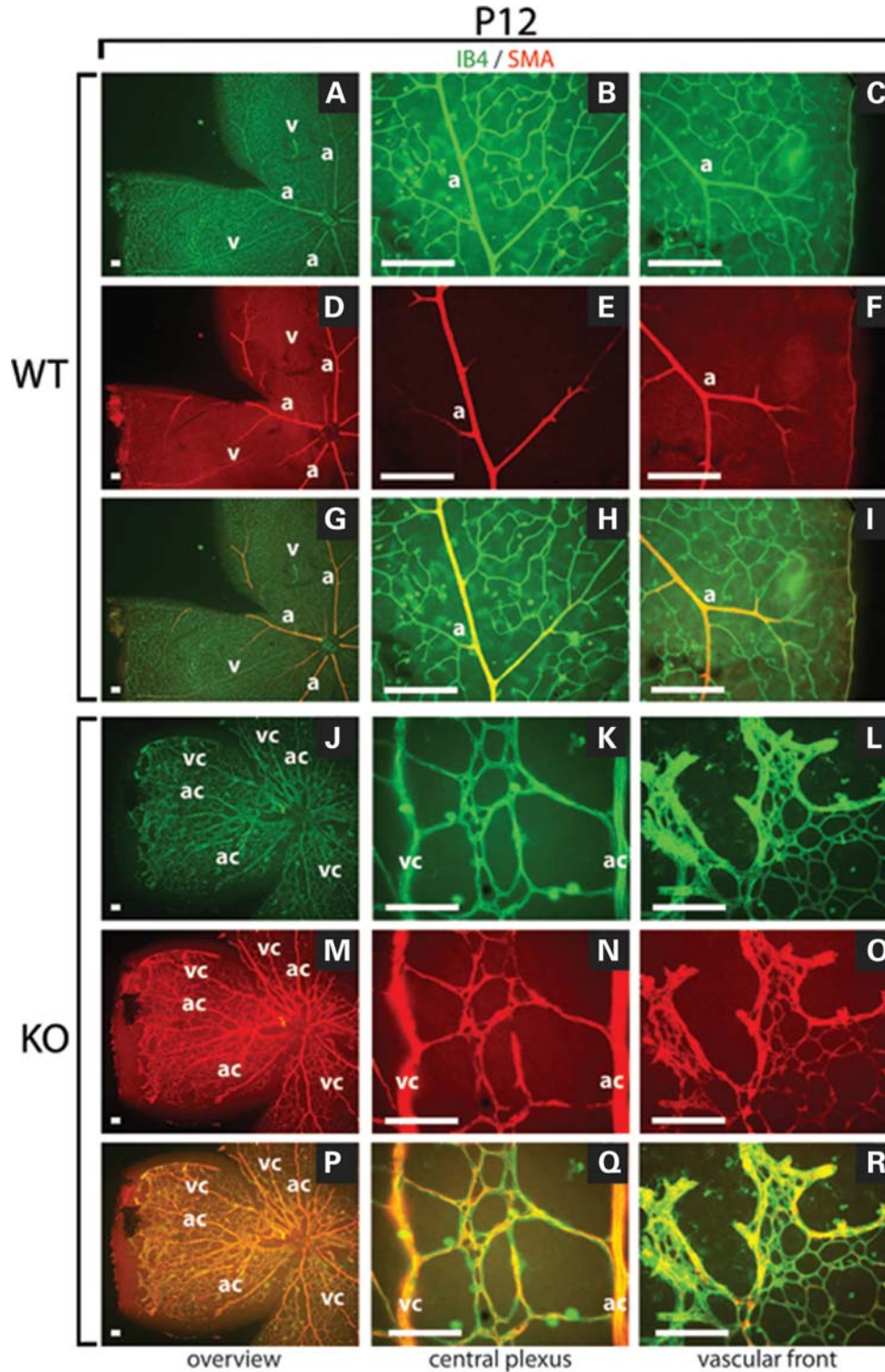


Figure 7. Retinal veins and capillaries are abundantly covered by mural cells (MCs) in *Ndp*^{−/−} mice at P12. Retinal whole-mounts were co-stained with IB4 to label blood vessels (green) and against SMA to label arteries covered by MCs (red). Only arteries were covered by MCs in wild-type (WT) retinas. In contrast, arteries, veins and capillaries were covered by MCs in *Ndp*^{−/−} retinas (KO). a, artery; ac, arterial character; v, vein; vc, venous character. Scale bars = 100 μm.

Further, we observed extensive crossing of arteries and veins (A/V) in *Ndp*^{−/−} retinas and we excluded an altered astrocytic scaffold to be the reason for these observations (Supplementary Material, Fig. S2).

Loss of Norrin signaling might alter MAPK signaling

A/V crossing is a feature of all Norrin-Wnt signaling deficient mice and also (12,13,16,24,25) the lack of the cytoplasmatic

domain of Nrp1 (*Nrp1*^{cytoΔ/Δ}) or dosage-dependent reduction in neuronal VEGF-A paracrine signaling (VEGF-A_{NES-CRE}) lead to A/V crossing (24,25). The receptor pair consisting of VEGFR2 and Nrp1 triggers VEGF-mediated downstream MAPK signaling. Thus, the existence of A/V crossing in *Ndp*^{y/y} retinas and in retinas from VEGF-A_{NES-CRE} and *Nrp1*^{cytoΔ/Δ} mice suggests that both pathways influence each other. Supporting this, Norrin-stimulated cells have elevated MAPK signaling activity compared with cells stimulated with mutant Norrin (Fig. 5I). Similarly, we previously reported MAPK signaling to be the major pathway influenced by Norrin signaling according to transcriptome analyses using microarray data from *Ndp*^{y/y} retinas (18). Therefore, it will be intriguing to investigate the putative link between Norrin-Wnt and VEGF/Nrp1/MAPK signaling.

Norrin stimulates mitogenic activity in retinal ECs

Since the loss of Norrin leads to delayed and incomplete outgrowth of the SRVP, we analyzed the mitogenic activity of Norrin in mouse retinas and in cell culture using systemic BrdU injection and reporter assays, respectively. The reduced proliferation of IB4-positive ECs from the SRVP in *Ndp*^{y/y} retinas, as revealed after BrdU injection, indicates that Norrin might act as a mitogenic stimulus (Fig. 3). Additionally, we monitored cell cycle progression by using the pE2F luciferase reporter construct. As expected, HEK293T cells, which endogenously express FZD4, LRP5 and TSPAN12 but not Norrin, and ectopically express human wild-type Norrin had an increased cell cycle progression compared with ectopically p.C95R mutant Norrin expressing cells (Fig. 3F). Consistently, Ohlmann *et al.* (35) observed, by using a BrdU ELISA, that Norrin efficiently stimulates proliferation of human retinal microvascular ECs *in vitro* in a Wnt-dependent manner. Our findings together with the BrdU ELISA suggest that Norrin might act as a mitogenic stimulus on microvascular/capillary ECs of the SRVP (Fig. 3C). This also can explain the delayed outgrowth of the SRVP. A key to understand the complexity of the retinal vascular phenotype in *Ndp*^{y/y} mice could be the differentiated view of events at the angiogenic front and within the central plexus. Transient peripheral phenomena like local hotspots of proliferation and remodeling, thickening of the vasculature and supernumerary filopodia could be interpreted as inability of vascular sprouts to escape the existing plexus. Hence, filopodia-projecting tip cells could be overrun by stalk cells, cluster and form the observed bulky areas. The supposed explanation for the *Ndp*^{y/y} superficial plexus phenotype is also supported by *in silico* models of vascular network formation. Travasso *et al.* (36) recently found, utilizing a mathematical model of sprouting angiogenesis, that low tip cell motility leads to a sparsely ramified plexus and increased stalk cell proliferation. Due to the lack of long tip cell protrusions projecting into the avascular space ahead of the vascular front, also characteristic for *Ndp*^{y/y} mice, stalk cells spend more angiogenic factors which decrease its concentrations and inhibits branching. The same study highlights that low overall EC proliferation also leads to reduced vessel ramification, corroborating our observations.

Veins and capillaries of *Ndp*^{y/y} retinas possess supernumerary central filopodia

To investigate the properties of ACs and VCs, we stained retinal whole-mounts against endomucin and SMA.

The surface of veins and capillaries in *Ndp*^{y/y} retinas was laced with endomucin-positive filopodia instead of being smooth and covered with none or very few filopodia as in control mice. The abundance of central filopodia peaks around P9, exactly when deep vascular sprouting in wild-type mice occurs. Interestingly, deep sprouting exclusively originates from venous vessels and capillaries but not from arteries. Therefore, it seems that veins and capillaries of the SRVP from *Ndp*^{y/y} retinas are able to create misaligned central filopodia. However, these filopodia might not be functional, since *Ndp*^{y/y} mice lack deep sprouting. It is also unclear which molecular mechanisms lead to those central supernumerary filopodia since published data focuses exclusively on the regulation of tip cell filopodia.

Veins and capillaries of *Ndp*^{y/y} retinas are excessively covered by MCs

Staining of retinal blood vessels for SMA revealed extensive MC coverage of veins and capillaries from P9 onwards. This coverage persists at least till P21. We previously reported upregulation of *PDGFβ* and *PDGFRβ* within the same timeframe (14). Interaction of all these genes regulates MC recruitment. Here, overexpression of *PDGFβ* and its receptor (*PDGFRβ*) could stimulate MC recruitment and the missing upregulation of *Ang1* on MCs might prevent restriction of MC recruitment. Considering this as the likely mechanism of the excessive MC recruitment, we believe that this might be a response to vessel leakiness caused by upregulation of *VEGF-A* and *PLVAP* (14,18) due to hypoxia. Currently, it is unclear if this extensive MC recruitment goes along with a gain of AC in the affected veins and venules. If so, the gain in arterial or loss of VC could explain the disability to form the DRVP out of the SRVP from *Ndp*^{y/y} retinas, since deep sprouts emerge exclusively from venous vessels and capillaries of the SRVP (37). The fact that we still can morphologically distinguish ACs and VCs and that we detected supernumerary endomucin-positive central filopodia on veins, venules and capillaries, but not on arteries, argues against a complete loss of the VC. However, the formation of uncoordinated central endomucin-positive filopodia at P9 and the excessive MC recruitment of venous vessels may indicate at least a partial loss of venous identity of the respective ECs with the consequence that central tip cells might develop, but being unable to induce proper deep sprouting.

The morphometric analysis together with results from the DAPT injections does not suggest a direct link between Norrin-Wnt and Notch signaling via Jag1. Our results suggest that Norrin is a mitogenic stimulus for IB4-positive ECs of the SRVP which explains its delayed outgrowth in *Ndp*^{y/y} mice. The A/V crossing occurs unlikely due to a disturbed astrocyte-EC interaction and it is unclear if the altered basal membrane of the SRVP contributes to this effect. We found that Norrin is able to stimulate MAPK signaling and also previously reported that MAPK signaling

might be the primarily altered pathway in Norrin KO retinas. All this together with the A/V crossing phenotype suggests that MAPK signaling might be significantly altered in Norrin KO retinas. We also found excessive MC coverage of veins, venules and capillaries in *Ndp^{v/-}* retinas which might indicate a partial loss of venous identity but also contribute to the appearance of the altered basal lamina and possibly to the appearance of the thorn-like supernumerary central filopodia. Postnatal stages after P7 in mice mimic developmental stages from patients when hypoxia increases and leads to pathologic alterations of various retinal angiogenic maturation processes. These data are crucial for the investigation of related diseases, like familial exudative vitreoretinopathy or Coats' disease, with a less severe phenotype than Norrie disease, which have a realistic chance for the development of treatment regimens.

MATERIALS AND METHODS

Animals

Generation of the *Ndp^{v/-}* mouse line has been described elsewhere (4). The research was performed in accordance with the ARVO Statement for the Use of Animals in Ophthalmic and Vision Research and was approved by the Veterinary Office of the State of Zurich (Switzerland).

Immunohistochemical staining

Retinas for whole-mount immunohistochemistry were fixed in 4% paraformaldehyde for 2 h or overnight at 4°C. After fixation, retinas were blocked using 1–10% normal goat or rabbit serum (VectorLabs) in PBST and subsequently incubated overnight with biotinylated IB4 (1:200; VectorLabs). The following primary antibodies were diluted in 1–5% serum in PBST and incubated over night: α SMA-CY3 (1:500; Sigma), ColIV (AbD serotec, 1:200), PDGFR α (R&D Systems, 1:500) and Endomucin (R&D Systems, 1:100). For secondary detection, Alexa Fluor streptavidin conjugates (Molecular Probes, 1:100) or anti-goat/rabbit Alexa Fluor-coupled secondary antibodies (Invitrogen, 1:500) were used. Retinas were washed five times with PBS, flat mounted and analyzed under bright-light illumination with a microscope (Axioplan 2, AxioCam HRc; Carl Zeiss) equipped with ApoTome (Carl Zeiss) or by confocal imaging using the CLSM Leica SP2 inverse microscope (Leica). The protocol from Pitulescu *et al.* (46) was used to stain for proliferating ECs (BrdU staining).

Image processing

Image J 1.44p (NIH) and Photoshop CS5 (Adobe) software were used for image processing. Overall image brightness was adjusted in a linear fashion on whole images if it was necessary to improve picture quality for prints. These adjustments did not influence interpretation and are in concert with suggestions for image processing in reference (38). Results shown were obtained by performing at least two different independent experiments including at least four mutant or control animals per stage.

Morphometric analysis of retinal flatmounts

Each morphometric parameter was determined by averaging over four non-overlapping images per retina (one retina used per animal) with a minimum of four animals per group. Vascular density was determined by measuring the endothelial coverage per 300 \times 300 μ m field at the vascular front. The number of branch points was determined by counting vessel branch points within 300 \times 300 μ m fields. The number of filopodia at the vascular front within 68 \times 51 μ m fields was counted and normalized to 100 μ m length of vasculature. BrdU-positive endothelial nuclei were counted in 424 \times 317 μ m fields at the vascular front and normalized to endothelial coverage within the same field (21).

In vivo Notch inhibition

Notch signaling was inhibited by subcutaneous injection of 0.3 mg/g body weight N-[N-(3,5-Difluorophenacetyl-L-alanyl)]-S-phenylglycine t-butylester (DAPT, Merck) dissolved in 10% ethanol and 90% peanut oil. DAPT solution was injected twice at P5 and P6. Retinas were collected at P7. Control litters were injected with vehicle only. Seven litters were DAPT injected. Quantification of vascular density and number of filopodia in DAPT-treated versus untreated KO and WT mice were performed as described above (23).

Quantification of Norrin-dependent proliferation and MAPK signaling in vitro

Stably wild-type or mutant p.C95R Norrin expressing HEK293T cells were used in these assays. Equal expression levels of wild-type and mutant Norrin were determined by western blot analysis (data not shown). To examine the proliferation rate or MAPK signaling activity, 8 \times 10⁴ cells/well of a 24-well plate were seeded and incubated at 37°C/5% CO₂ overnight. Cells were transiently co-transfected with pE2F or pSRF firefly luciferase reporter and pRenilla constructs (SABiosciences) using the calcium precipitation method (39,40). Luciferase activity was measured using DualGlo-LuciferaseReporterAssaySystem (Promega). Firefly luciferase activity was normalized to co-transfected *Renilla* luciferase.

Statistical analysis

Statistical analysis was performed in SPSS 18.0 (IBM) using two-tailed unpaired Student's *t*-test.

Quantitative data from DAPT-injection experiments were processed with univariate analysis of variance with two independent variables. Avoiding bias due to unequal sample sizes, the estimated marginal means were calculated instead of arithmetically means. *P*-values below $\alpha = 0.05$ were considered significant.

SUPPLEMENTARY MATERIAL

Supplementary Material is available at *HMG* online.

ACKNOWLEDGEMENTS

We thank Britta Seebauer for contributing the immunostainings against α -SMA at P7. We also would like to thank Rui Bedito, Ralf Adams and Hiroyuki Yamamoto for giving practical advice and discussing this work as well as Wei Chi for donating the pFZD4 construct and He Xi and Bryan McDonalds for providing the pLRP5 construct.

Conflict of Interest statement. None declared.

FUNDING

This work was supported by the Velux Foundation, Zurich, Switzerland and by the Swiss National Science Foundation (Grant number 31003A_122359), Bern, Switzerland.

REFERENCES

- Berger, W., Meindl, A., van de Pol, T.J., Cremers, F.P., Ropers, H.H., Doerner, C., Monaco, A., Bergen, A.A., Lebo, R. and Warburg, M. (1992) Isolation of a candidate gene for Norrie disease by positional cloning. *Nat. Genet.*, **1**, 199–203.
- Berger, W., van de Pol, D., Warburg, M., Gal, A., Bleeker-Wagemakers, L., de Silva, H., Meindl, A., Meitingner, T., Cremers, F. and Ropers, H.H. (1992) Mutations in the candidate gene for Norrie disease. *Hum. Mol. Genet.*, **1**, 461–465.
- Warburg, M. (1966) Norrie's disease. A congenital progressive oculo-acoustico-cerebral degeneration. *Acta Ophthalmol. (Copenh.)*, **85 (suppl.)**, 5–147.
- Berger, W., van de Pol, D., Bachner, D., Oerlemans, F., Winkens, H., Hameister, H., Wieringa, B., Hendriks, W. and Ropers, H.H. (1996) An animal model for Norrie disease (ND): gene targeting of the mouse ND gene. *Hum. Mol. Genet.*, **5**, 51–59.
- Chen, Z.Y., Battinelli, E.M., Fielder, A., Bunday, S., Sims, K., Breakefield, X.O. and Craig, I.W. (1993) A mutation in the Norrie disease gene (NDP) associated with X-linked familial exudative vitreoretinopathy. *Nat. Genet.*, **5**, 180–183.
- Shastri, B.S., Hejtmancik, J.F. and Trese, M.T. (1997) Identification of novel missense mutations in the Norrie disease gene associated with one X-linked and four sporadic cases of familial exudative vitreoretinopathy. *Hum. Mutat.*, **9**, 396–401.
- Black, G.C., Perveen, R., Bonshek, R., Cahill, M., Clayton-Smith, J., Lloyd, I.C. and McLeod, D. (1999) Coats' disease of the retina (unilateral retinal telangiectasis) caused by somatic mutation in the NDP gene: a role for norrin in retinal angiogenesis. *Hum. Mol. Genet.*, **8**, 2031–2035.
- Shastri, B.S., Pendergast, S.D., Hartzler, M.K., Liu, X. and Trese, M.T. (1997) Identification of missense mutations in the Norrie disease gene associated with advanced retinopathy of prematurity. *Arch. Ophthalmol.*, **115**, 651–655.
- Ye, X., Wang, Y. and Nathans, J. (2010) The Norrin/Frizzled4 signaling pathway in retinal vascular development and disease. *Trends Mol. Med.*, **16**, 417–425.
- Nikopoulos, K., Gilissen, C., Hoischen, A., van Nouhuys, C.E., Boonstra, F.N., Blokland, E.A., Arts, P., Wieskamp, N., Strom, T.M., Ayuso, C. et al. (2010) Next-generation sequencing of a 40 Mb linkage interval reveals TSPAN12 mutations in patients with familial exudative vitreoretinopathy. *Am. J. Hum. Genet.*, **86**, 240–247.
- Poulter, J.A., Ali, M., Gilmour, D.F., Rice, A., Kondo, H., Hayashi, K., Mackey, D.A., Kearns, L.S., Ruddle, J.B., Craig, J.E. et al. (2010) Mutations in TSPAN12 cause autosomal-dominant familial exudative vitreoretinopathy. *Am. J. Hum. Genet.*, **86**, 248–253.
- Xu, Q., Wang, Y., Dabdoub, A., Smallwood, P.M., Williams, J., Woods, C., Kelley, M.W., Jiang, L., Tasman, W., Zhang, K. and Nathans, J. (2004) Vascular development in the retina and inner ear: control by Norrin and Frizzled-4, a high-affinity ligand-receptor pair. *Cell*, **116**, 883–895.
- Junge, H.J., Yang, S., Burton, J.B., Paes, K., Shu, X., French, D.M., Costa, M., Rice, D.S. and Ye, W. (2009) TSPAN12 regulates retinal vascular development by promoting Norrin- but not Wnt-induced FZD4/ beta-catenin signaling. *Cell*, **139**, 299–311.
- Luhmann, U.F., Lin, J., Acar, N., Lammel, S., Feil, S., Grimm, C., Seeliger, M.W., Hammes, H.P. and Berger, W. (2005) Role of the Norrie disease pseudoglioma gene in sprouting angiogenesis during development of the retinal vasculature. *Invest. Ophthalmol. Vis. Sci.*, **46**, 3372–3382.
- Richter, M., Gottanka, J., May, C.A., Welge-Lüssen, U., Berger, W. and Lutjen-Drecoll, E. (1998) Retinal vasculature changes in Norrie disease mice. *Invest. Ophthalmol. Vis. Sci.*, **39**, 2450–2457.
- Xia, C.H., Yablonka-Reuveni, Z. and Gong, X. (2010) LRP5 is required for vascular development in deeper layers of the retina. *PLoS ONE*, **5**, e11676.
- Rehm, H.L., Zhang, D.S., Brown, M.C., Burgess, B., Halpin, C., Berger, W., Morton, C.C., Corey, D.P. and Chen, Z.Y. (2002) Vascular defects and sensorineural deafness in a mouse model of Norrie disease. *J. Neurosci.*, **22**, 4286–4292.
- Schafer, N.F., Luhmann, U.F., Feil, S. and Berger, W. (2009) Differential gene expression in Ndp-knockout mice in retinal development. *Invest. Ophthalmol. Vis. Sci.*, **50**, 906–916.
- Liebner, S., Corada, M., Bangsow, T., Babbage, J., Taddei, A., Czupalla, C.J., Reis, M., Felici, A., Wolburg, H., Fruttiger, M. et al. (2008) Wnt/ beta-catenin signaling controls development of the blood-brain barrier. *J. Cell Biol.*, **183**, 409–417.
- Gerhardt, H., Golding, M., Fruttiger, M., Ruhrberg, C., Lundkvist, A., Abramsson, A., Jeltsch, M., Mitchell, C., Alitalo, K., Shima, D. and Betsholtz, C. (2003) VEGF guides angiogenic sprouting utilizing endothelial tip cell filopodia. *J. Cell Biol.*, **161**, 1163–1177.
- Lobov, I.B., Renard, R.A., Papadopoulos, N., Gale, N.W., Thurston, G., Yancopoulos, G.D. and Wiegand, S.J. (2007) Delta-like ligand 4 (Dll4) is induced by VEGF as a negative regulator of angiogenic sprouting. *Proc. Natl Acad. Sci. USA*, **104**, 3219–3224.
- Benedito, R., Roca, C., Sorensen, I., Adams, S., Gossler, A., Fruttiger, M. and Adams, R.H. (2009) The notch ligands Dll4 and Jagged1 have opposing effects on angiogenesis. *Cell*, **137**, 1124–1135.
- Hellstrom, M., Phng, L.K., Hofmann, J.J., Wallgard, E., Coultas, L., Lindblom, L., Alva, J., Nilsson, A.K., Karlsson, L., Gaiano, N. et al. (2007) Dll4 signalling through Notch1 regulates formation of tip cells during angiogenesis. *Nature*, **445**, 776–780.
- Fantin, A., Schwarz, Q., Davidson, K., Normando, E.M., Denti, L. and Ruhrberg, C. (2011) The cytoplasmic domain of neuropilin 1 is dispensable for angiogenesis, but promotes the spatial separation of retinal arteries and veins. *Development*, **138**, 4185–4191.
- Haigh, J.J., Morelli, P.I., Gerhardt, H., Haigh, K., Tsien, J., Damert, A., Miquerol, L., Muhlner, U., Klein, R., Ferrara, N. et al. (2003) Cortical and retinal defects caused by dosage-dependent reductions in VEGF-A paracrine signaling. *Dev. Biol.*, **262**, 225–241.
- Katoh, M. and Katoh, M. (2006) Notch ligand, JAG1, is evolutionarily conserved target of canonical WNT signaling pathway in progenitor cells. *Int. J. Mol. Med.*, **17**, 681–685.
- Estrach, S., Ambler, C.A., Lo, C.C., Hozumi, K. and Watt, F.M. (2006) Jagged 1 is a beta-catenin target gene required for ectopic hair follicle formation in adult epidermis. *Development*, **133**, 4427–4438.
- Singh, S., Johnson, J. and Chellappan, S. (2010) Small molecule regulators of Rb-E2F pathway as modulators of transcription. *Biochim. Biophys. Acta*, **1799**, 788–794.
- Isashiki, Y., Ohba, N., Yanagita, T., Hokita, N., Doi, N., Nakagawa, M., Ozawa, M. and Kuroda, N. (1995) Novel mutation at the initiation codon in the Norrie disease gene in two Japanese families. *Hum. Genet.*, **95**, 105–108.
- Baluk, P., Morikawa, S., Haskell, A., Mancuso, M. and McDonald, D.M. (2003) Abnormalities of basement membrane on blood vessels and endothelial sprouts in tumors. *Am. J. Pathol.*, **163**, 1801–1815.
- Baffert, F., Le, T., Sennino, B., Thurston, G., Kuo, C.J., Hu-Lowe, D. and McDonald, D.M. (2006) Cellular changes in normal blood capillaries undergoing regression after inhibition of VEGF signaling. *Am. J. Physiol. Heart Circ. Physiol.*, **290**, H547–H559.
- Liu, C., Shao, Z.M., Zhang, L., Beatty, P., Sartippour, M., Lane, T., Livingston, E. and Nguyen, M. (2001) Human endomucin is an endothelial marker. *Biochem. Biophys. Res. Commun.*, **288**, 129–136.
- Samulowitz, U., Kuhn, A., Brachtendorf, G., Nawroth, R., Braun, A., Bankfalvi, A., Bocker, W. and Vestweber, D. (2002) Human endomucin: distribution pattern, expression on high endothelial venules, and decoration with the MECA-79 epitope. *Am. J. Pathol.*, **160**, 1669–1681.

34. Chen, J., Stahl, A., Krah, N.M., Seaward, M.R., Dennison, R.J., Sapieha, P., Hua, J., Hatton, C.J., Juan, A.M., Aderman, C.M. *et al.* (2011) Wnt signaling mediates pathological vascular growth in proliferative retinopathy. *Circulation*, **124**, 1871–1881.
35. Ohlmann, A., Seitz, R., Braunger, B., Seitz, D., Bosl, M.R. and Tamm, E.R. (2010) Norrin promotes vascular regrowth after oxygen-induced retinal vessel loss and suppresses retinopathy in mice. *J. Neurosci.*, **30**, 183–193.
36. Travasso, R.D., Poiré, E.C., Castro, M., Rodríguez-Manzaneque, J.C. and Hernandez-Machado, A. (2011) Tumor angiogenesis and vascular patterning: a mathematical model. *PLoS ONE*, **6**, e19989.
37. Fruttiger, M. (2007) Development of the retinal vasculature. *Angiogenesis*, **10**, 77–88.
38. Rossner, M. and Yamada, K.M. (2004) What's in a picture? The temptation of image manipulation. *J. Cell Biol.*, **166**, 11–15.
39. Jordan, M., Schallhorn, A. and Wurm, F.M. (1996) Transfecting mammalian cells: optimization of critical parameters affecting calcium-phosphate precipitate formation. *Nucleic Acids Res.*, **24**, 596–601.
40. Jordan, M. and Wurm, F. (2004) Transfection of adherent and suspended cells by calcium phosphate. *Methods*, **33**, 136–143.
41. Xia, C.H., Liu, H., Cheung, D., Wang, M., Cheng, C., Du, X., Chang, B., Beutler, B. and Gong, X. (2008) A model for familial exudative vitreoretinopathy caused by LPR5 mutations. *Hum. Mol. Genet.*, **17**, 1605–1612.
42. Chen, J., Stahl, A., Krah, N.M., Seaward, M.R., Joyal, J.S., Juan, A.M., Hatton, C.J., Aderman, C.M., Dennison, R.J., Willett, K.L. *et al.* (2012) Retinal expression of wnt-pathway mediated genes in low-density lipoprotein receptor-related protein 5 (lrp5) knockout mice. *PLoS ONE*, **7**, e30203.
43. Phng, L.K., Potente, M., Leslie, J.D., Babbage, J., Nyqvist, D., Lobov, I., Ondr, J.K., Rao, S., Lang, R.A., Thurston, G. and Gerhardt, H. (2009) Nrarp coordinates endothelial Notch and Wnt signaling to control vessel density in angiogenesis. *Dev. Cell*, **16**, 70–82.
44. Gale, N.W., Thurston, G., Hackett, S.F., Renard, R., Wang, Q., McClain, J., Martin, C., Witte, C., Witte, M.H., Jackson, D. *et al.* (2002) Angiopoietin-2 is required for postnatal angiogenesis and lymphatic patterning, and only the latter role is rescued by Angiopoietin-1. *Dev. Cell*, **3**, 411–423.
45. Caprara, C., Thiersch, M., Lange, C., Joly, S., Samardzija, M. and Grimm, C. (2011) HIF1A is essential for the development of the intermediate plexus of the retinal vasculature. *Invest. Ophthalmol. Vis. Sci.*, **52**, 2109–2117.
46. Pitulescu, M.E., Schmidt, I., Benedito, R. and Adams, R.H. (2010) Inducible gene targeting in the neonatal vasculature and analysis of retinal angiogenesis in mice. *Nat. Protoc.*, **5**, 1518–1534.